ChemComm

COMMUNICATION

View Article Online
View Journal | View Issue

Cite this: *Chem. Commun.*, 2016, 52, 10652

Received 31st May 2016,
Accepted 1st August 2016

DOI: 10.1039/c6cc04538c

www.rsc.org/chemcomm

Hollow silica nanospheres coated with insoluble calcium salts for pH-responsive sustained release of anticancer drugs†

Yuming Guo,*[ab] Qilong Fang,[a] Han Li,[a] Weike Shi,[a] Jie Zhang,[a] Jing Feng,[a] Weili Jia[a] and Lin Yang*[ab]

Hollow silica nanospheres coated with biocompatible and pH-sensitive inorganic insoluble calcium salts including calcium carbonate and hydroxyapatite have been successfully prepared. The results indicate that the nanospheres can efficiently load doxorubicin and release it in a pH-responsive and sustained manner, and improve the treatment efficacy significantly.

At present, the treatment efficacy of chemotherapeutic drugs is far from satisfactory because of poor specificity and serious side effects.[1,2] Therefore, drug delivery systems (DDSs) have attracted tremendous attention on account of significant improvement in efficacy and diminishment of side effects.[3,4] Recently, hollow silica nanospheres (HSNSs) have been considered as an important drug delivery platform.[5,6] To employ HSNSs as drug carrier, it is critical to release the drug in a controlled manner to targeted sites.[7] Unfortunately, owing to poor sensitivity to physiological environmental changes and sudden release behavior, pristine HSNSs may not be directly applied as carriers for the controlled release of anticancer drugs.[8] It is well known that tumor tissues have a lower local pH (*ca.* 5–6) than normal tissues (*ca.* 7.4),[9] which can be exploited as the drug-release trigger for pH-sensitive carriers. Theoretically, the release of the drugs loaded in HSNSs can be triggered by this pH difference to avoid uncontrolled release.[10,11] Therefore, the pristine HSNSs have generally been coated by pH-sensitive polymers to improve the pH-dependent release performance.[12–14] However, the complicated preparation of the pH-sensitive polymers and the potential cytotoxicity of the degradation products have significantly limited the practical applications.

Compared with polymer coatings, inorganic coatings show significant advantages, *e.g.* facile synthesis, better biocompatibility, and good degradability. Because of the good biocompatibility and pH-sensitivity of calcium carbonate ($CaCO_3$)[15,16] and hydroxyapatite (HAP),[17] their potential application as coatings of HSNSs to achieve the sustained controlled release of anticancer drugs attracts our interest.

Herein, HSNSs coated with $CaCO_3$ (SiO_2–$CaCO_3$) and HAP (SiO_2–HAP) were prepared and used as anticancer drug carriers, in which pH-sensitive $CaCO_3$ and HAP could control the drug release. The results revealed that SiO_2–$CaCO_3$ and SiO_2–HAP could efficiently load doxorubicin (DOX). In addition, the drug-loaded carriers could be specifically internalized by cancer cells and release DOX in a sustained controlled manner in response to the weak acidic microenvironment of cancer cells. These attributes resulted in the significant enhancement of the anticancer effect of DOX. The results presented here suggest that HSNSs coated with pH-sensitive inorganic materials might be used as DDSs to treat human cancers efficiently.

In the current study, using freshly prepared polystyrene nanospheres (PSNSs) with average diameter of 377 nm as hard template (Fig. S1a, ESI†), PS/SiO_2–NH_2 nanospheres were prepared through the hydrolysis of tetraethylorthosilicate (TEOS). Then, SiO_2–NH_2 hollow nanospheres were prepared through elimination of the PS cores. Subsequently, SiO_2–COOH hollow nanospheres were obtained by acetic anhydride treatment. Afterwards, SiO_2–$CaCO_3$ and SiO_2–HAP hybrid hollow nanospheres were synthesized by means of the absorption of Ca^{2+} onto the surface of the SiO_2–COOH hollow nanospheres and the subsequent addition of Na_2CO_3 and $(NH_4)_2HPO_4$ (Scheme 1). Then, DOX was loaded onto the nanospheres (SiO_2–$CaCO_3$/DOX and SiO_2–HAP/DOX). SiO_2–$CaCO_3$/DOX and SiO_2–HAP/DOX were delivered to cancer cells and specifically internalized by cancer cells through passive targeted delivery of SiO_2–$CaCO_3$/DOX and SiO_2–HAP/DOX utilizing the enhanced permeability and retention (EPR) effect. Finally, the $CaCO_3$ and HAP layer of SiO_2–$CaCO_3$/DOX and SiO_2–HAP/DOX, respectively, was decomposed within the acidic microenvironment of the cancer cell to release the DOX to treat the cancer.

[a] *Collaborative Innovation Center of Henan Province for Green Manufacturing of Fine Chemicals, Key Laboratory of Green Chemical Media and Reactions, Ministry of Education, Henan Normal University, Xinxiang, Henan 453007, P. R. China. E-mail: guoyuming@htu.edu.cn, yanglin1819@163.com*

[b] *Henan Key Laboratory of Green Chemical Media and Reactions, School of Chemistry and Chemical Engineering, Henan Normal University, Xinxiang, Henan 453007, P. R. China*

† Electronic supplementary information (ESI) available: Experimental details and supplementary results. See DOI: 10.1039/c6cc04538c

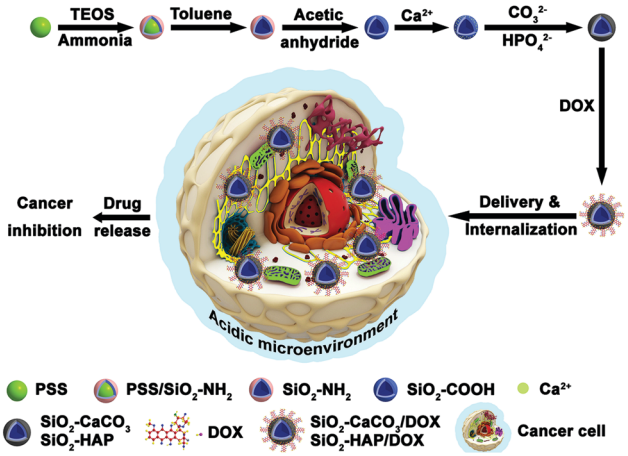

Scheme 1 Mechanism for the preparation of SiO_2–$CaCO_3$ and SiO_2–HAP hybrid hollow nanospheres and the application in drug loading, delivery, sustained release and cancer treatment of SiO_2–$CaCO_3$/DOX, and SiO_2–HAP/DOX.

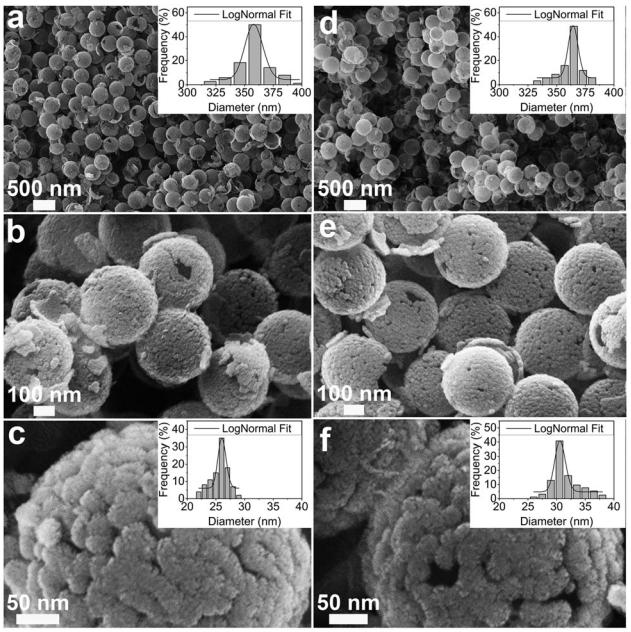

Fig. 1 FE-SEM images of (a–c) SiO_2–$CaCO_3$ and (d–f) SiO_2–HAP hollow nanospheres. Insets: Size distribution analysis results.

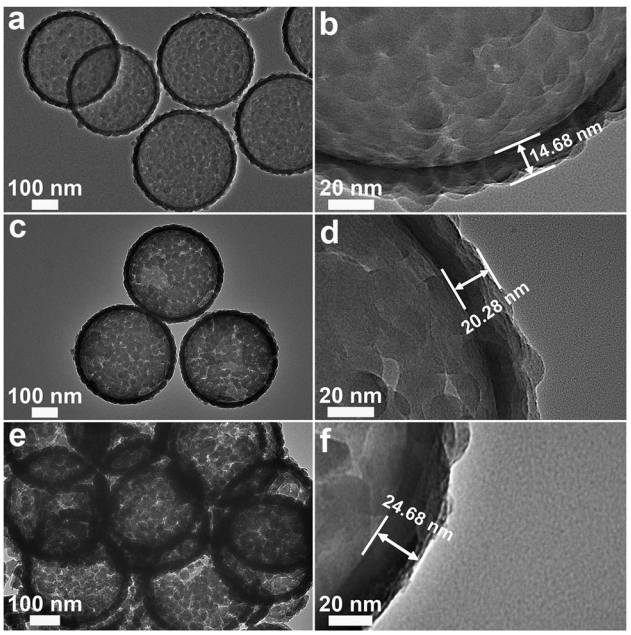

Fig. 2 HR-TEM images of (a and b) SiO_2–COOH, (c and d) SiO_2–$CaCO_3$ and (e and f) SiO_2–HAP hollow nanospheres.

The morphology and size of the products were determined by field emission scanning electron microscopy (FE-SEM). In Fig. S1b (ESI†), PS/SiO_2 is seen as well-dispersed spheres with average diameter 385 nm, slightly larger than PSNSs. This can be attributed to the deposition of SiO_2 onto the PSNS surface. After elimination of the PS cores, the morphology of the sample is preserved, also showing ideal spheres, with average diameter of 355 nm (Fig. S1c, ESI†) indicating slight shrinkage during toluene treatment. After treated with acetic anhydride, the SiO_2 surface was coated with –COOH groups. In Fig. S1d (ESI†), SiO_2–COOH is seen as well-dispersed spheres with average diameter of 351 nm.

Using SiO_2–COOH hollow nanospheres as hard template, SiO_2–$CaCO_3$ and SiO_2–HAP were prepared. From the results, SiO_2–$CaCO_3$ are well-dispersed hollow nanospheres with average diameter of 358 nm (Fig. 1a). The broken spheres show the hollow feature. From Fig. 1d, SiO_2–HAPs are also well-dispersed hollow nanospheres with average diameter 364 nm, slightly larger than SiO_2–$CaCO_3$. From FE-SEM observations, SiO_2–$CaCO_3$ and SiO_2–HAP are composed of nanoclusters with average sizes of 26 nm (Fig. 1b and c) and 31 nm (Fig. 1e and f).

From high-resolution transmission electron microscopy (HR-TEM) observation, the shell thickness of SiO_2–COOH is about 14.68 nm (Fig. 2a and b). In comparison, the shell thickness of SiO_2–$CaCO_3$ increases to 20.28 nm, of which the thickness of the $CaCO_3$ coating layer is calculated to be 5.60 nm (Fig. 2c and d). The shell thickness of SiO_2–HAP is about 24.68 nm, of which the thickness of the HAP coating layer is about 10.00 nm (Fig. 2e and f).

The presence of $CaCO_3$ and HAP layers in SiO_2–$CaCO_3$ and SiO_2–HAP was confirmed by X-ray diffraction (XRD) analysis. From Fig. 3a, compared with SiO_2–COOH, the XRD pattern of SiO_2–$CaCO_3$ exhibits weak diffraction peaks of (104), (110), and (113) planes of calcite.[18] The weakness of the diffraction peaks can be attributed to the poor crystallinity. When SiO_2 is removed through NaOH treatment, the XRD pattern shows the clear diffraction peaks of the calcite. The XRD pattern of SiO_2–HAP also exhibits a similar phenomenon (Fig. 3b). Additionally, the selected area electron diffraction (SAED) patterns and energy dispersive X-ray (EDX) spectra also indicate the presence of $CaCO_3$ and HAP (Fig. S2. ESI†). These results confirm the successful deposition of $CaCO_3$ or HAP layers onto the surface of SiO_2–COOH. Based on the molecular structure, the amino group in DOX assigns it a net positive charge.[19] From the literature, high drug-loading

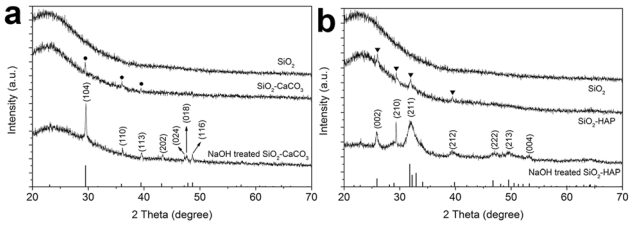

Fig. 3 XRD patterns of (a) SiO_2, SiO_2–$CaCO_3$, and NaOH treated SiO_2–$CaCO_3$ hollow nanospheres and (b) SiO_2, SiO_2–HAP and NaOH treated SiO_2–HAP hollow nanospheres.

capacity and loading efficiency can be achieved through the charge interactions of the carriers with the drugs.[20,21] Moreover, an ideal drug carrier should be negatively charged or uncharged in the physiological environment to reduce toxicity and prolong blood circulation time.[22,23] From ξ-potential data (Fig. 4a), SiO_2–NH_2 carries positive charge under physiological conditions, unfavorable to the loading of the positive DOX. However, ξ-potential changes to negative after the surface modification of SiO_2–NH_2. Furthermore, through the surface coating of SiO_2–COOH with $CaCO_3$ and HAP, ξ-potential changes to yet more negative. This result suggests that SiO_2–$CaCO_3$ and SiO_2–HAP, with negative ξ-potentials, might possess better DOX loading capacity and efficiency than SiO_2–NH_2 and SiO_2–COOH. The drug loading evaluation showed that SiO_2–$CaCO_3$ and SiO_2–HAP could efficiently load DOX (Fig. 4b and c) and the DOX degrees of entrapment of SiO_2–NH_2, SiO_2–COOH, SiO_2–$CaCO_3$, and SiO_2–HAP are 15.73%, 36.91%, 90.34%, and 94.12%, respectively. The DOX loading efficiencies (wt%) of SiO_2–NH_2, SiO_2–COOH, SiO_2–$CaCO_3$, and SiO_2–HAP are 1.57%, 3.69%, 9.03%, and 9.41%, respectively (Fig. S4, ESI†). This confirms the better DOX loading performance of SiO_2–$CaCO_3$ and SiO_2–HAP.

Generally, the acidic microenvironment of tumor tissues can be used as drug-release stimulus for pH-sensitive DDSs. Therefore, the *in vitro* release performances of SiO_2–$CaCO_3$/DOX and SiO_2–HAP/DOX were evaluated in buffers with different pH simulating tumor and normal tissues. From Fig. 4d and e, the release performances of SiO_2–$CaCO_3$/DOX and SiO_2–HAP/DOX under acidic conditions are much better than those under normal physiological conditions. On the one hand, this can be ascribed to the gradual decomposition of $CaCO_3$ and HAP under acidic conditions, which is confirmed by the obvious morphological changes of SiO_2–$CaCO_3$ and SiO_2–HAP in acidic release buffers (Fig. S5 and S6, ESI†). In addition, the better solubility of DOX in acidic solution also contributes to the pH-triggered drug release of DOX. This suggests that SiO_2–$CaCO_3$ and SiO_2–HAP might be used as pH-sensitive carriers to release drugs in response to the acidic microenvironment of tumors. Additionally, DOX release occurs in an obviously sustained manner over a period of 5 days for SiO_2–$CaCO_3$/DOX and 8 days for SiO_2–HAP/DOX. These systems can exert their anticancer activity for much longer duration than the pure counterpart and reduce the administration frequency.

For a chemotherapeutic drug, the specificity can be defined as the IC_{50} ratio between normal and cancer cells.[18] A higher

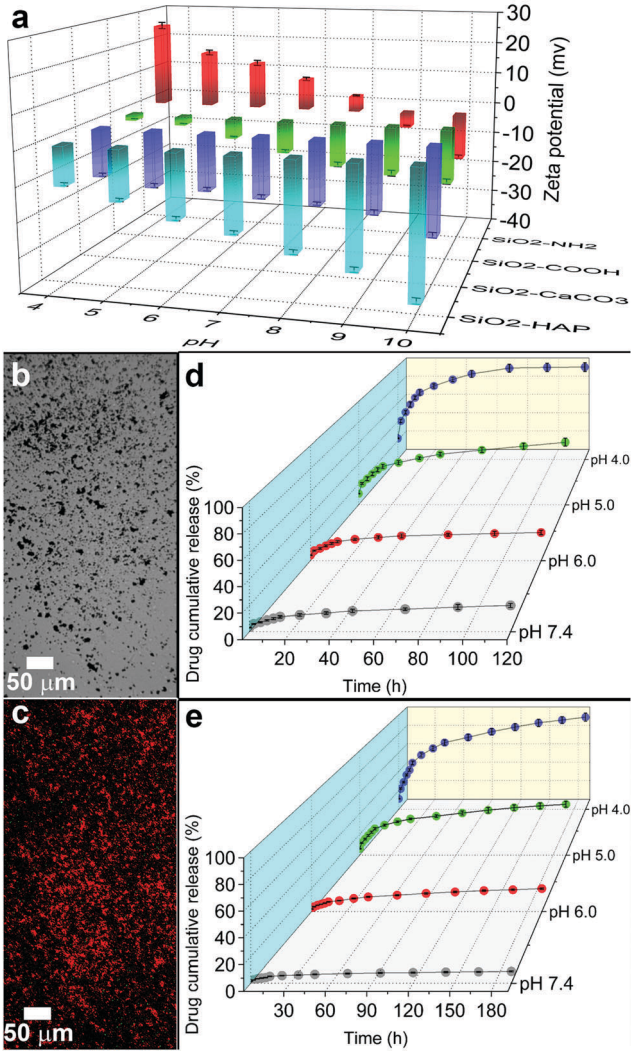

Fig. 4 (a) ξ-Potentials of the SiO_2–NH_2, SiO_2–COOH, SiO_2–$CaCO_3$, and SiO_2–HAP hollow nanospheres. (b) Light and (c) fluorescence micrographs of SiO_2–$CaCO_3$/DOX. The red autofluorescence of DOX is used to monitor its loading into SiO_2–$CaCO_3$. *In vitro* pH-responsive release profiles of (d) SiO_2–$CaCO_3$/DOX and (e) SiO_2–HAP/DOX under different pH values. Each data point represents the mean ± S.D., n = 6.

ratio represents better specificity. From the results shown in Fig. 5a, after treatment for 3 days, the IC_{50} values of DOX, SiO_2–$CaCO_3$/DOX, and SiO_2–HAP/DOX for V79-4 normal cells are 0.2127, 0.5671, and 0.4736 μg mL^{-1}, respectively. This indicates an obvious reduction of the undesirable side effects of DOX on normal cells. The IC_{50} values of DOX, SiO_2–$CaCO_3$/DOX, and SiO_2–HAP/DOX for Hep G2 cancer cells are 0.1542, 0.1128, and 0.1215 μg mL^{-1}, respectively (Fig. 5b). This reveals the efficient augmentation of the anticancer effect of DOX after being loaded onto SiO_2–$CaCO_3$ and SiO_2–HAP. Based on these data, the specificities of the free DOX, SiO_2–$CaCO_3$/DOX, and SiO_2–HAP/DOX are calculated as 1.3794, 5.0275, and 3.8979, respectively. It is notable that the specificity of DOX is significantly improved by 3.64-fold and 2.83-fold through loading onto SiO_2–$CaCO_3$ and SiO_2–HAP. This indicates that SiO_2–$CaCO_3$ and SiO_2–HAP can significantly enhance the specificity and treatment

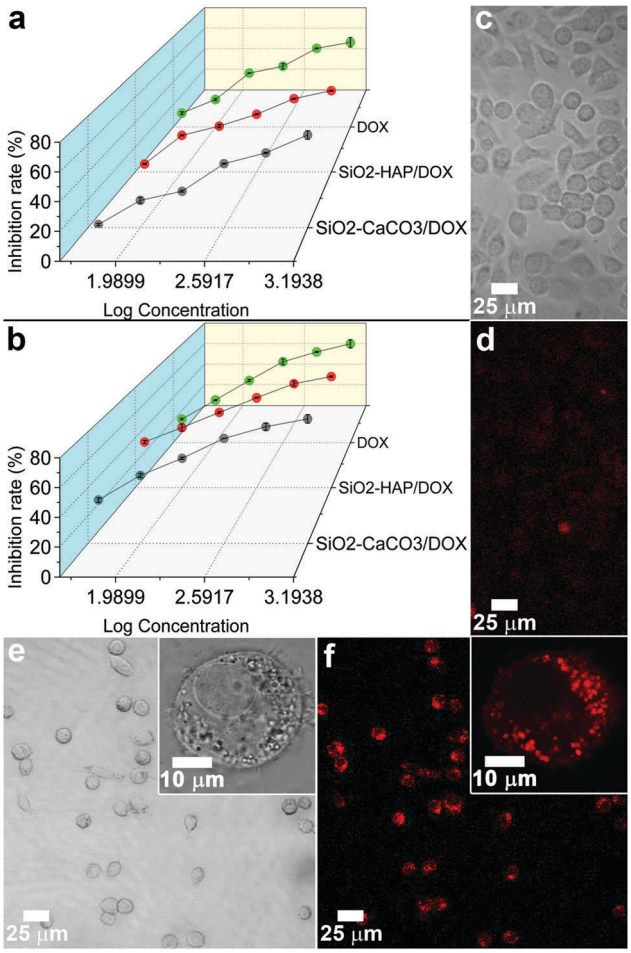

Fig. 5 Cytotoxic effects of free DOX, SiO_2–$CaCO_3$/DOX, and SiO_2–HAP/DOX on (a) V79-4 and (b) Hep G2 cells after 3 days of treatment. Each data point represents the mean ± S.D., n = 6. (c) Light and (d) fluorescence micrographs of V79-4 normal cells and (e and f) Hep G2 cancer cells after treatment with SiO_2–$CaCO_3$/DOX for 48 h. Insets: Magnified images.

efficacy of DOX. From the microscopy images of the normal cells and cancer cells after treatment with SiO_2–$CaCO_3$/DOX for 48 h (Fig. 5c and e), the cell density of the cancer cells is significantly lower than that of the normal cells, confirming the specific and significant inhibition of the cancer cells. Furthermore, after treatment with SiO_2–$CaCO_3$/DOX for 48 h, just a few of the normal cells emit the weak red fluorescence of DOX (Fig. 5d). However, all the cancer cells emit strong red fluorescence after treatment with SiO_2–$CaCO_3$/DOX (Fig. 5f). More importantly, the presence of aggregates of SiO_2–$CaCO_3$/DOX in the cancer cells is clearly seen (insets of Fig. 5e and f). This indicates that SiO_2–$CaCO_3$/DOX can be specifically internalized by cancer cells rather than by normal cells, which might be attributed to the passive targeted delivery of SiO_2–$CaCO_3$/DOX utilizing the EPR effect. It is this passive targeted delivery of SiO_2–$CaCO_3$/DOX and SiO_2–HAP/DOX that results in the significant enhancement of the anticancer effect of DOX.

In summary, HSNSs coated with biocompatible and pH-sensitive $CaCO_3$ and HAP were prepared successfully through a facile method. The characteristics of the SiO_2–$CaCO_3$ and SiO_2–HAP, including the pH-sensitivity of $CaCO_3$ and HAP and the much more negative charge, endow them with effective loading capacity, pH-responsiveness and sustained release of anticancer drugs to specifically treat human cancers. Based on these findings, HSNSs modified by pH-sensitive inorganic coatings might be used as the DDS to treat human cancers efficiently.

This work was financially supported by the National Natural Science Foundation of China (21271066, 21171051, and U1204516) and Program for Science & Technology Innovation Talents in Universities of Henan Province (13HASTIT011) and Key Young Teachers Project of Henan Province (2012GGJS-065).

Notes and references

1 L. Cabeza, R. Ortiz, J. L. Arias, J. Prados, M. A. Ruiz Martínez, J. M. Entrena, R. Luque and C. Melguizo, *Int. J. Nanomed.*, 2015, **10**, 1291–1306.
2 Q. He and J. Shi, *Adv. Mater.*, 2014, **26**, 391–411.
3 R. Duan, F. Xia and L. Jiang, *ACS Nano*, 2013, **7**, 8344–8349.
4 M. Vallet-Regí, F. Balas and D. Arcos, *Angew. Chem., Int. Ed.*, 2007, **46**, 7548–7558.
5 E. Climent, R. Martínez-Máñez, F. Sancenón, M. D. Marcos, J. Soto, A. Maquieira and P. Amorós, *Angew. Chem., Int. Ed.*, 2010, **49**, 7281–7283.
6 F. Tang, L. Li and D. Chen, *Adv. Mater.*, 2012, **24**, 1504–1534.
7 C.-Y. Lai, B. G. Trewyn, D. M. Jeftinija, K. Jeftinija, S. Xu, S. Jeftinija and V. S. Y. Lin, *J. Am. Chem. Soc.*, 2003, **125**, 4451–4459.
8 B. G. Trewyn, I. I. Slowing, S. Giri, H.-T. Chen and V. S. Y. Lin, *Acc. Chem. Res.*, 2007, **40**, 846–853.
9 M. Stubbs, P. M. J. McSheehy, J. R. Griffiths and C. L. Bashford, *Mol. Med. Today*, 2000, **6**, 15–19.
10 L. Du, S. Liao, H. A. Khatib, J. F. Stoddart and J. I. Zink, *J. Am. Chem. Soc.*, 2009, **131**, 15136–15142.
11 Y. Gao, Y. Chen, X. Ji, X. He, Q. Yin, Z. Zhang, J. Shi and Y. Li, *ACS Nano*, 2011, **5**, 9788–9798.
12 B. Chang, D. Chen, Y. Wang, Y. Chen, Y. Jiao, X. Sha and W. Yang, *Chem. Mater.*, 2013, **25**, 574–585.
13 C.-C. Huang, W. Huang and C.-S. Yeh, *Biomaterials*, 2011, **32**, 556–564.
14 C. Yang, W. Guo, L. Cui, N. An, T. Zhang, H. Lin and F. Qu, *Langmuir*, 2014, **30**, 9819–9827.
15 T.-Y. Cheang, S.-M. Wang, Z.-J. Hu, Z.-H. Xing, G.-Q. Chang, C. Yao, Y. Liu, H. Zhang and A.-W. Xu, *J. Mater. Chem.*, 2010, **20**, 8050–8055.
16 F. He, J. Zhang, F. Yang, J. Zhu, X. Tian and X. Chen, *Mater. Sci. Eng., C*, 2015, **50**, 257–265.
17 Y.-H. Yang, C.-H. Liu, Y.-H. Liang, F.-H. Lin and K. C. W. Wu, *J. Mater. Chem. B*, 2013, **1**, 2447–2450.
18 Y. Guo, J. Zhang, L. Jiang, X. Shi, L. Yang, Q. Fang, H. Fang, K. Wang and K. Jiang, *Chem. Commun.*, 2012, **48**, 10636–10638.
19 Z. Wang, G. Ma, J. Zhang, W. Lin, F. Ji, M. T. Bernards and S. Chen, *Langmuir*, 2014, **30**, 3764–3774.
20 H. Deng, J. Liu, X. Zhao, Y. Zhang, J. Liu, S. Xu, L. Deng, A. Dong and J. Zhang, *Biomacromolecules*, 2014, **15**, 4281–4292.
21 A. F. Jimenez-Kairuz, D. A. Allemandi and R. H. Manzo, *Int. J. Pharm.*, 2004, **269**, 149–156.
22 J.-Z. Du, X.-J. Du, C.-Q. Mao and J. Wang, *J. Am. Chem. Soc.*, 2011, **133**, 17560–17563.
23 Z. Kang, C. H. A. Tsang, Z. Zhang, M. Zhang, N.-B. Wong, J. A. Zapien, Y. Shan and S.-T. Lee, *J. Am. Chem. Soc.*, 2007, **129**, 5326–5327.